J Math Chem (2009) 46:971–980
DOI 10.1007/s10910-009-9549-x

ORIGINAL PAPER

A parallel study of $Ni@Si_{12}$ and $Cu@Si_{12}$ nanoclusters

A. D. Zdetsis · E. N. Koukaras · C. S. Garoufalis

Received: 9 September 2006 / Accepted: 30 September 2008 / Published online: 16 July 2009

Abstract The $Ni@Si_{12}$ and $Cu@Si_{12}$ clusters are studied in parallel within the framework of the density functional theory using the hybrid functional of Becke-Lee, Parr and Yang (B3LYP), emphasizing the differences and similarities in structural and electronic properties. The dominant structures for both clusters are a distorted hexagonal structure of C_s symmetry and a distorted octahedral structure of D_{2d}. For $Ni@Si_{12}$ the two structures are practically isonergetic whereas for $Cu@Si_{12}$ the energy difference of the D_{2d} structure from the lowest C_s structure of hexagonal origin is about 0.7 eV, at the B3LYP/TZVP level of theory. Contrary to $Cu@Si_{12}$ for which the well known Frank–Kasper (FK) structure of C_{5v} symmetry is a real local minimum of the energy hyper-surface (although higher by more than 1.6 eV from the global minimum), for $Ni@Si_{12}$ the FK structure is dynamically unstable. The HOMO-LUMO gaps, the binding energies per atom and the embedding energies for $Cu@Si_{12}$ clusters are smaller by 0.5, 0.1 and 1.1 eV, respectively compared to the $Ni@Si_{12}$ clusters. This is attributed to different type of bonding in the two clusters.

Keywords Metal encapsulated clusters · Nanocluster · Silicon · Transition metal · Ab initio calculations

1 Introduction

Over the last 2 decades the research on silicon and silicon-based materials has grown tremendously for obvious technological and scientific reasons. In contrast to carbon, silicon cannot easily form stable cages and fullerenes, which are favored by the sp^2 hybridization. In the late 1980s Beck [1,2] found that silicon clusters doped with

A. D. Zdetsis (✉) · E. N. Koukaras · C. S. Garoufalis
Department of Physics, University of Patras, 26500 Patras, Greece
e-mail: zdetsis@upatras.gr; zdetsis@physics.upatras.gr

transition metal atoms (TMA) exhibit increased stability compared to the corresponding pure silicon clusters. This initiated intense interest on TMA encapsulated Si clusters for promising applications in nanotechnology and nanoscience. It is known by now that advancements in the electronics industry have led to silicon based integrated circuits with elements (MOSFETS) as small as a few nanometers. It is anticipated that stable silicon clusters may serve as building blocks for the construction of novel nanoscale silicon based materials with a tunable band gap, depending on the encapsulated TMA.

Within this perspective, a subject of great concern is the chemistry that occurs at the interface between a metal and a silicon surface. It has been speculated [1,2] that metal-containing stable silicon clusters may represent the earliest products formed at the interface.

In the early work of Beck [1,2] three types of TMA were used; specifically Tungsten (W), Molybdenum (Mo) and Chromium (Cr). Hiura et al. [3] reported later that TMAs react with silane (SiH_4) producing Si clusters with an encapsulated TM atom. The TMA interaction with the silicon network, considered to be endohedral, stabilizes the Si cage. The TMAs that react with SiH_4 to form stable cages have a partially filled d-shell with more than two d electrons in the ground state. It was discovered that the $TM@Si_n$ clusters that were formed, lost their reactivity to SiH_4 when n reached 12, suggesting that $TM@Si_{12}$ constitute stable clusters.

From a theoretical point of view, the structural stability and electronic properties of $TM@Si_n$ clusters have been heavily investigated the last few years with a large variety of theoretical methods [4–12]. The use of *ab initio* theoretical methods for the determination of structural and electronic properties is by no means a trivial task. The difficulties involved can be readily appreciated considering that even for small pure Si clusters (which have been under investigation for many years) there are still numerous fundamental issues to be resolved [13–15]. The incorporation of TMAs introduces partially filled d-electrons (and possible different spin states) that makes the situation even more complex, leading some times to discrepancies and controversies.

Although Ni is very effective for stabilizing carbon cages, the theoretical work for Ni-doping of silicon clusters, such as $Ni@Si_{12}$ is rather limited, compared to $Cu@Si_{12}$ and other TMA-embedded silicon clusters. Menon et al. [6] have performed a series of TBMD as well as DFT calculations in an effort to identify the energetically more stable isomer of $Ni@Si_{12}$. The results of both theoretical approximations in Ref. [6], suggest that the lowest energy Ni-encapsulated Si structure is a cage of C_{5v} symmetry. This conclusion has been questioned by Kumar [9] who suggests that the structure of C_{5v} symmetry of Menon et al. is the third lowest in energy, while two other structures, a distorted hexagonal prism and a chair structure are energetically more favorable. The present work attempts to resolve this and other controversies, examining in parallel both the $Ni@Si_{12}$ and the $Cu@Si_{12}$ clusters with high accuracy methods. Furthermore, the comparison could help the understanding and the distinction of the embedded-silicon clusters characteristics, which are due to the partial filling of d-shells, with those that are not so strongly dependent on the [spd] hybridization (the dominant electronic configuration is $[Ar]3d^84s^2$, for Ni and $[Ar]3d^{10}4s^1$, for Cu).

2 Technical details

Several different approaches were adopted for the construction of the initial candidate geometries, independent of the ones existing in the literature (except for the hexagonal prism and the Frank–Kasper (FK) C_{5v} symmetric structure). We started by considering ideal fcc and hcp cells, as well as two additional structures of hexagonal and icosahedral symmetry. In all cases we performed symmetry unconstrained (C_1) geometry optimizations, using the gradient corrected BP86 [16,17] functional with the SVP [18] basis set. At this stage of the calculations the resolution of the identity (RI) [19] approximation for the two-electron integrals was consistently employed. After "symmetrization" the 6 lowest energetically structure were re-optimized using the hybrid three parameter, non-local correlation functional Becke-Lee, Parr and Yang (B3LYP) [20] with the large triple-zeta quality split valence basis set TZVP [21]. Based upon prior experience [14,15] the B3LYP functional gives exceptionally accurate results for both electronic [13–15] and structural properties for Si. Moreover, for the case of silicon clusters [13], it has been shown that the quality of B3LYP results is comparable to more sophisticated and computationally demanding methods, such as CCSD(T). For the TMA containing structures the B3LYP functional yields accurate binding energies, but rather short bond lengths [22,23]. This procedure was followed for Ni and then the same structures were optimized in the same way for Cu. Well known and well established structures for Cu [4] were not examined any further, since the purpose of the study was the comparison of the less-studied Ni clusters with well-studied Cu clusters. The geometric and electronic configuration of the clusters was determined by additional stability calculations, by performing calculations on different spin states (singlet, triplet, etc.), by employing occupation number optimization procedures using (pseudo-Fermi) thermal smearing and by comparing to other high level methods, when it was considered necessary. The bulk of our calculations were performed using the Turbomole [24] program package.

3 Results and discussion

3.1 Structural and bonding characteristics

Our calculations for $Ni@Si_{12}$ reveal two distinct, nearly isoenergetic lowest energy structures, of C_s symmetry and D_{2d} symmetry, respectively. The C_s structure, shown in Fig. 2a, was proposed by Kumar [9] as the lowest energy structure for the $Ni@Si_{12}$ cluster, instead of the FK C_{5v} structure proposed by Menon et al. [6], in Fig. 1f. The D_{2d} structure in Fig. 2b, to the best of our knowledge, has not been identified before as a stable isomer of the $Ni@Si_{12}$ cluster. The C_s isomer could be regarded as a hexagonal prism in which a single Si atom has elongated bond lengths in the case of Ni, and two Si atoms with elongated bond lengths in the case of Cu. The D_{2d} structure can be regarded as four distorted neighboring pentagons. This structure was obtained straightforward by the optimization procedure using as an initial geometry an hcp unit cell (including first and second neighbors of the central Ni atom), ending up to the structure of Fig. 2b. In the case of the C_s isomer the structure used

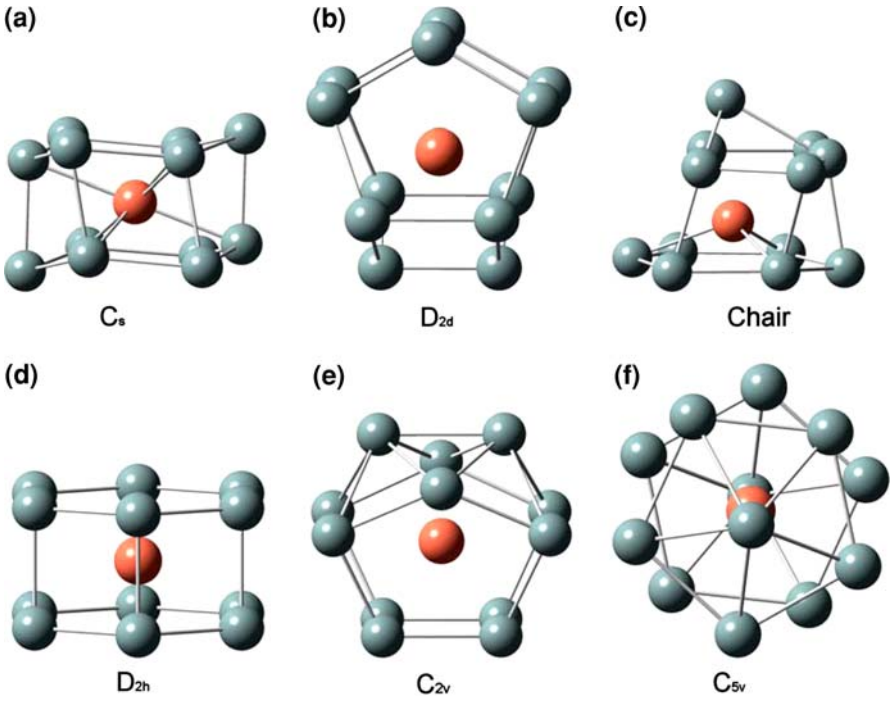

Fig. 1 The six lowest lying isomers of the $Cu@Si_{12}$ cluster (the Cu atom at the *center*). We show the (**a**) distorted hexagonal prism C_s (**b**) fullerene-like D_{2d} (**c**) chair-like C_s (**d**) hexagonal prism D_{2h} (**e**) C_{2v} and (**f**) Frank-Kasper C_{5v} structures. Similar structures exist for $Ni@Si_{12}$

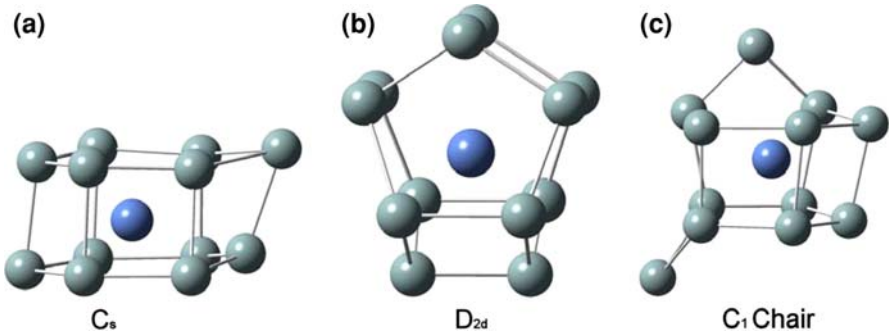

Fig. 2 The three energetically lowest isomers of the $Ni@Si_{12}$ cluster (the Ni atom at the *center*). We show the (**a**) distorted hexagonal prism C_s (b) fullerene-like D_{2d} and (**c**) chair-like C_1 structures. Three additional structures are similar to those of $Cu@Si_{12}$, specifically Fig. 1d-f, and are not reproduced here

as the initial geometry was a hexagonal prism of tight D_{2h} symmetry, as shown in Fig. 1d. This nearly hexagonal structure is known to be stable for most of the TMAs [5]. However, in the case of Ni frequency calculations revealed three imaginary values. By performing a continuous cyclic procedure of distorting the successive structure in accordance to the imaginary frequencies, we ended up with the distorted hexagonal

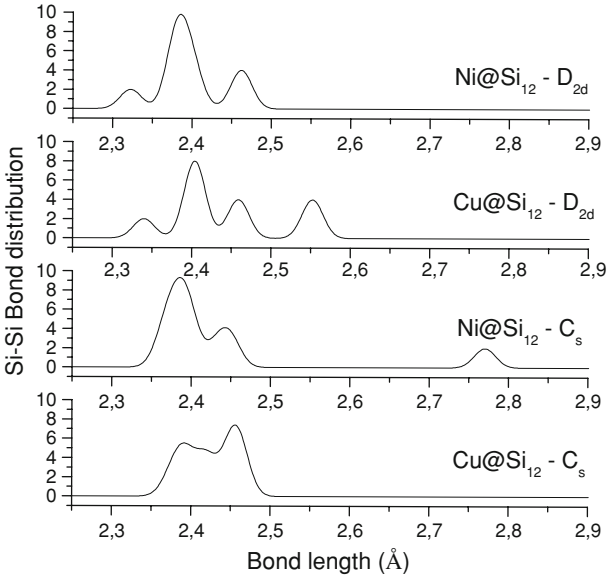

Fig. 3 Comparison of the bond-length distribution (in arbitrary units) of Si–Si bonds for the C_s and D_{2d} structures. Bond-lengths are in Å

prism in Fig. 2a of C_s symmetry. Finally, the chair structure in Fig. 2c of near C_s symmetry (C_s with loose symmetry criteria) was obtained by consecutive C_1 (symmetry unconstrained) optimizations of the C_{5v} isomer.

The analogous structures for Cu, shown in Fig. 1, have somewhat different characteristics, but overall the same symmetry and structural origin. The differences and similarities for the two lowest structures can be easily appreciated from the bond-length distributions of Fig. 3. In Fig. 3 the bond-length distribution of the silicon bonds for the C_s and D_{2d} structures is displayed for both $Ni@Si_{12}$ and $Cu@Si_{12}$ clusters. As we can see, the $Cu@Si_{12}$ C_s cluster is more symmetric (limited range of bond-lengths), without long silicon bonds (there is no peak at about 2.77 Å). This must also be reflected in the electronic and cohesive characteristics. The higher average symmetry of the corresponding Cu-structures compared to those of Ni is a general characteristics seen for all structures. For instance, the D_{2h} structure of $Ni@Si_{12}$ cluster, which with strict symmetry criteria is actually C_{2h}, corresponds (with loose symmetry criteria) to a near D_{6h} hexagonal prism for the $Cu@Si_{12}$ cluster. This must be related to the spherical symmetry of the complete 3d shell in the copper atom. It should be emphasized that both C_s structures (being the lowest energetically for each of the two clusters) have resulted from distortions of the original hexagonal prism, which has very high stability for all TMA-doped clusters [5]. However, the Jahn-Teller distortions are expected to lower the symmetry, as in the present case for Ni and Cu. Otherwise, the dynamical stability of the structures should be tested by vibrational analysis. Such analysis for the high symmetry structures for Ni of Fig. 1d and f indeed reveals imaginary frequencies.

The bond distribution diagrams reflect the tendency of Ni (but also of Cu) to have 10 nearest neighbors, instead of 12, as can be also inferred by the non-convex structures

of the energetically lowest isomers shown in Figs. 1 and 2. This is in agreement with Andriotis et al. [25] who illustrated that stable Si nanotubes constructed by using higher Z 3d-transition metals prefer a distorted structure of C_{5v} symmetry, in which each Ni atom has 10 nearest neighbors. Nevertheless, the C_{5v} isomer for $Ni@Si_{12}$, as was shown here is dynamically unstable. This indicates that the stability of the C_{5v} nanotube is rather inherent and is not derived from the C_{5v} nanocluster.

3.2 Cohesive and electronic characteristics

In Table 1 we have summarized several cohesive and electronic characteristics for the structures of Figs. 1 and 2 (i.e. for both $Ni@Si_{12}$ and $Cu@Si_{12}$ clusters). These include total energies, relative energies with respect to the lowest energy structure, ΔE, binding energies per atom, BE/atom, HOMO-LUMO gaps, HL, and embedding energies, EE and EE2.

The embedding energy measures the ability of the particular TMA to stabilize a silicon cluster. This quantity is defined as the difference of the total energy from the sum of the energy of hollow silicon cage energy and the energy of the TMA:

$$\mathrm{EE} = [E(\mathrm{Si}_n)_{hc} + E(\mathrm{TM})] - E(\mathrm{TM@Si}_n).$$

There are alternative ways of defining EE (for instance, in place of the hollow (non-relaxed) silicon structure energy $E(\mathrm{Si}_n)_{hc}$, one can consider the energy of the energetically lowest Si cluster). For our purposes, the definition above is enough, but nevertheless we provide calculations based on both definitions for comparison with the literature. We can observe that, although the binding energies per atom of $Ni@Si_{12}$ compared to $Cu@Si_{12}$ are better by only about 0.1 eV for all structures, the corresponding embedding energies are far better by more than 1.4 (up to 1.8) eV, which illustrates the ability of Ni to stabilize silicon cages much better than Cu. The deeper reason for this will be examined in a different work. The higher HL gaps in $Ni@Si_{12}$ (by about 0.5 eV) also verify this stability. As we can see in Fig. 4, the HOMOs are dominated by silicon (sp) states, for both $Cu@Si_{12}$ and $Ni@Si_{12}$ with a slightly higher d-state contribution in the case of Ni (for the C_s isomer). This is in agreement with the findings of Ref. [11] for an increasing d-character in the HOMO orbitals in going from Cu to Ni. This is also partly true for the corresponding LUMOs (see Fig. 5). For the C_s structure the succession of positive and negative values and the general nodal pattern suggests that the LUMO orbitals are of anti-bonding character. Again, this is partly true for the LUMO orbitals. Also, the observations for the hybridization character of the orbitals are clearer for the C_s structure (ground state for both metal systems), compared to the D_{2d}. Specifically, for the C_s isomer, the contribution of the Ni atom to the HOMO is approximately 7%, in contrast to the contribution of the Cu atom which is near zero (zero s and p contributions and marginal d contribution).

The small difference in binding energy could be attributed to the long bonds in $Ni@Si_{12}$ (see Fig. 3) which lower the binding energy of the silicon network; whereas the large difference in embedding energies must be related to the more inert 3d shell in Cu. We also observe that the C_s and D_{2d} structures in $Ni@Si_{12}$ are practically

Table 1 Energetic properties of the $Ni@Si_{12}$ and $Cu@Si_{12}$ clusters

Isomer	$Ni@Si_{12}$						$Cu@Si_{12}$					
	Energy (Ha)	ΔE (eV)	HL (eV)	BE/atom (eV/atom)	EE (eV)	EE2 (eV)	Energy (Ha)	ΔE (eV)	HL (eV)	BE/atom (eV/atom)	EE (eV)	EE2 (eV)
C_s	−4981.784	0.00	1.55	3.17	5.43	3.32	−5113.941	0.00	1.05	3.08	4.03	2.11
D_{2d}	−4981.783	0.04	1.60	3.17	6.02	3.28	−5113.914	0.74	1.13	3.02	4.25	1.37
Chair (Cs)	−4981.765	0.51	1.53	3.13	5.43	2.82	−5113.901	1.09	1.53	2.99	3.70	1.02
D_{2h}	−4981.765	0.52	1.02	3.13	5.44	2.80	−5113.893	1.32	0.42	2.97	3.57	0.80
C_{2v}	−4981.759	0.69	1.20	3.12	5.69	2.64	−5113.884	1.56	1.12	2.96	3.54	0.56
C_{5v}(FK)	−4981.708	2.06	1.16	3.01	4.49	1.26	−5113.880	1.66	1.39	2.95	3.96	0.45

Total energies, relative energies (ΔE), binding energies per atom (BE/atom), HOMO-LUMO gap (HL) and embedding energies (EE, EE2)

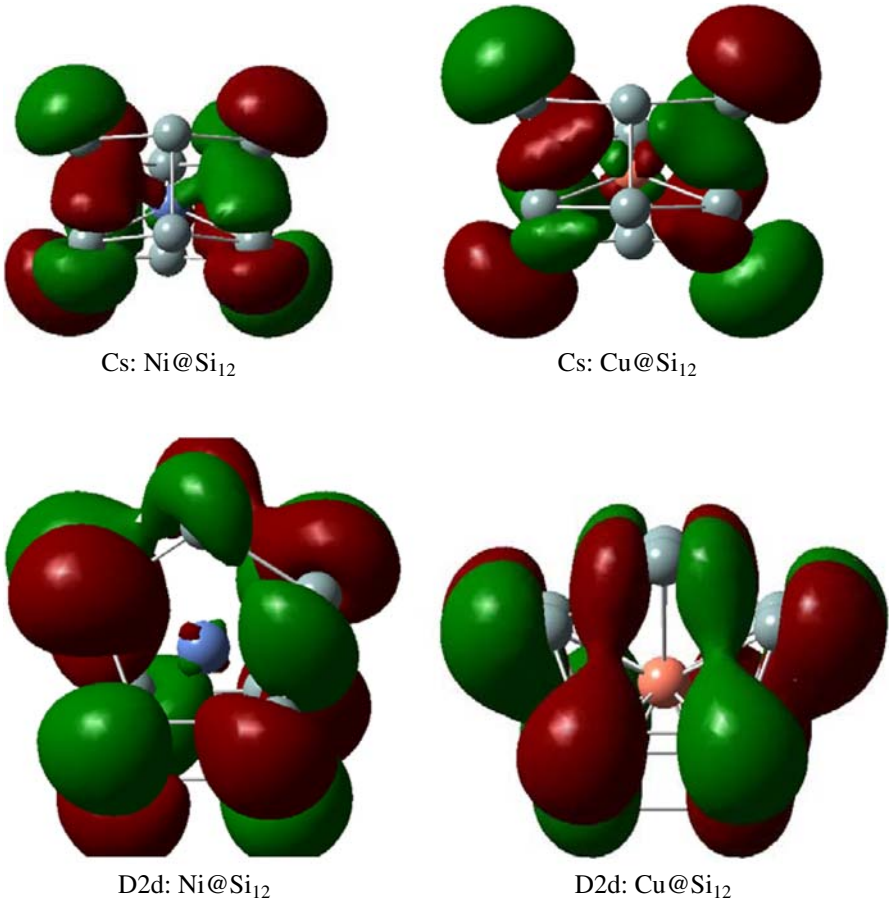

Fig. 4 Comparison of the highest occupied molecular orbitals (HOMO) for the D_{2d} and C_s structures

isoenergetic. This could be loosely interpreted as a competition between hexagonal and cubic building patterns (due to competing different sp-d hybridization patterns). As a matter of fact at different levels of theory the energy ordering of the C_s and D_{2d} structures is reversed in $Ni@Si_{12}$. In contrast, in $Cu@Si_{12}$ the energy difference of these two structures is high (1.4 eV). Moreover, in $Cu@Si_{12}$ the D_{2d} structure is not the second lowest in energy but the fourth, although its EE ranks higher than some of the lower structures [4]. We note that the energetically intermediate structures (from C_s and D_{2d}) the Cu atom is not endohedral (i.e. the structures are not cages).

4 Conclusions

It has been shown that although the C_s structure, resulting through the distortions of a highly symmetric hexagonal prism, constitutes the ground state geometry for both $Cu@Si_{12}$ and $Ni@Si_{12}$. At the B3LYP/TZVP level of theory, a "cubic" D_{2d}

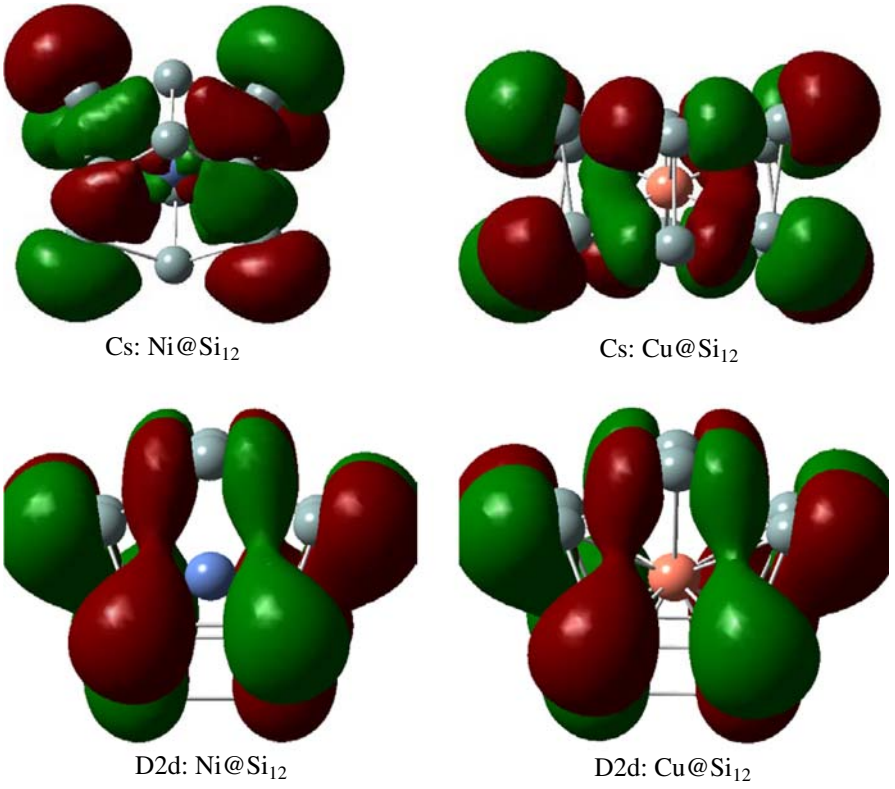

Fig. 5 Comparison of the lowest unoccupied molecular orbitals (LUMO) for the D_{2d} and C_s structures

dodecahedron is nearly isoenergetic for $Ni@Si_{12}$. At different levels of theory this structure could be lower than the "hexagonal" C_s structure. As would be expected on the basis of the 3d-shell filling of the metallic atoms, the embedding energies (and generally the cohesive characteristics) of $Ni@Si_{12}$ are much better than those of $Cu@Si_{12}$ due to stronger spd-hybridization (in the former). Different types of spd-hybridization in $Ni@Si_{12}$ lead to a competition between "hexagonal" and "cubic" structural patterns. The "chair" structure, suggested by Kumar et al. [9], is the third lowest structure with a 0.5 eV energy difference from the ground state. For both type of clusters the highly symmetric (C_{5v} symmetry) FK structure, is by more than 1.5 eV higher in energy from the lowest structure and it is dynamically unstable for $Ni@Si_{12}$. Further work on this subject is currently under way.

Acknowledgments We thank the University of Patras/Research Committee and particularly the basic research program "K. KARATHEODORI 2003" and the European Social Fund (ESF), Operational Program for Educational and Vocational Training II (EPEAEK II), and particularly the program PYTHAGORAS, for funding the above work.

References

1. S.M. Beck, J. Chem. Phys. **90**, 6306 (1989)
2. S.M. Beck, J. Chem. Phys. **87**, 4233 (1987)
3. H. Hiura, T. Miyazaki, T. Kanayama, Phys. Rev. Lett. **86**, 1733 (2001)
4. C. Xiao, F. Hagelberg, Phys. Rev. B **66**, 075425 (2002)
5. P. Sen, L. Mitas, Phys. Rev. B **68**, 155404 (2003)
6. M. Menon, A. Andriotis, G. Froudakis, Nano Lett. **2**, 301 (2002)
7. A.K. Singu, T.M. Briere, V. Kumar, Y. Kawazoe, Phys. Rev. Lett. **91**, 146802 (2003)
8. S.N. Khanna, B.K. Rao, P. Jena, Phys. Rev. Lett. **89**, 016803 (2002)
9. V. Kumar, Eur. Phys. J. D **24**, 227 (2003)
10. J. Lu, S. Nagase, Phys. Rev. Lett. **90**, 115506 (2003)
11. G. Mpourmpakis, G.E. Froudakis, A.N. Andriotis, M. Menon, Phys. Rev. B **68**, 125407 (2003)
12. V. Kumar, Comp. Mat. Sci. **30**, 260 (2004)
13. A.D. Zdetsis, Phys. Rev. A **64**, 023202 (2001)
14. A.D. Zdetsis, Rev. Adv. Mat. Sci. (RAMS) **11**, 56–78 (2006)
15. C.S. Garoufalis, A.D. Zdetsis, S. Grimme, Phys. Rev. Lett. **87**, 276402 (2001)
16. A.D. Becke, Phys. Rev. A **38**, 3098 (1988)
17. J.P. Perdew, Phys. Rev. B **33**, 8822 (1986)
18. A. Schäfer, H. Horn, R. Ahlrichs, J. Chem. Phys. **97**, 2571 (1992)
19. K. Eichkorn, O. Treutler, H. Öhm, M. Häser, R. Ahlrichs, Chem. Phys. Lett. **240**, 283 (1995)
20. P.J. Stephens, F.J. Devlin, C.F. Chabalowski, M.J. Frisch, J. Phys. Chem. **98**, 11623 (1994)
21. A. Schäfer, C. Huber, R. Ahlrichs, J. Chem. Phys. **100**, 5829 (1994)
22. P.J. Stephens, F.J. Devlin, C.F. Chabalowski, M.J. Frisch, J. Phys. Chem. **98**, 11623 (1994)
23. K. Yanagisawa, T. Tsuneda, K. Hirao, J. Chem. Phys. **112**, 545 (2000)
24. R. Ahlrichs, M. Bär, M. Häser, H. Horn, C. Kölmel. Chem. Phys. Lett. **162**, 165 (1989)
25. A.T. Andriotis, G. Mpourmpakis, G.E. Froudakis, M. Menon, New J. Phys. **4**, 78 (2002)